

EFFECT OF GAS TYPE ON FLOW CHARACTERISTICS IN A CIRCUIT BREAKER UNDER COLD FLOW SCENARIO

YUJIAO QIAO, SHANIKA MATHARAGE, ZHONGDONG WANG*

Centre for Smart Grid, Department of Engineering, University of Exeter, Exeter, United Kingdom, EX4 4PY

* zhongdong.wang@exeter.ac.uk

Abstract. This paper presents first stage of supersonic flow modelling in gas circuit breakers without an arc. Flow characterisation focused on shock and flow separation phenomenon. Velocity deceleration caused by shock will play a significant role in determining arc cooling performance and will impact thermal interruption capability. Gas properties such as specific heat ratio, density, and viscosity influenced the flow characteristics including shock location, strength and the flow separation process.

Keywords: gas circuit breakers, supersonic flow, shock, flow separation, gas properties.

1. Introduction

Gas circuit breaker (GCB) is an important component of the electrical power network. It is used to protect electrical equipment and to isolate faults in the system [1]. Due to excellent insulation and arc quenching properties (Sulphur hexa-fluoride) SF₆ is the most commonly used quenching medium in high voltage GCBs [1]. However, SF₆ has a very high global warming potential (GWP) and is a potent greenhouse gas. This has resulted in a worldwide investigation in environmentally friendly alternative gases for GCBs.

Modelling and simulation is an important tool to study flow behaviour under different conditions and optimize flow performance [2]. Besides, it is difficult to carry out flow characteristic during switching operations in the experiments [3]. The flow structure and flow characteristic are typically studied in ‘de Laval’ nozzle [4, 5], which is a convergent-divergent nozzle that allows exhaust gases to accelerate. Flow in nozzle experience acceleration from subsonic at inlet to sonic at nozzle throat, then reach supersonic at downstream area [6]. These rapid and extreme changes have a drastic impact on gas flow that leading to shocks and flow separation. Shock is characterised by a sudden pressure rise in the flow stream which leads to a sharp drop in the flow velocity [7]. Also under highly over expanded conditions, the flow stream at the solid boundaries cannot sustain the adverse pressure gradient and hence the flow separates from the nozzle wall, resulting in a shock at the separation base [8]. Such changes within the flow patterns have drastic impacts on the arc cooling process and eventually the arc quenching process. According to [9], when an arc is divided due to a shock, the voltage taken by the arc section after the shock will become negligible to the section before the shock. This will also decrease the effective arc length that can carry the recovery voltage. Therefore, the shock will eventually determine the effective arc length the region in which the thermal interruption will occur. It is vital for circuit breaker models to be able to predict such

phenomenon. This paper focuses on simulating the supersonic flow in a ‘de Laval’ nozzle and investigating the impact of gas types and contact position on the shock formation and flow separation process.

2. Methodology

2.1. Governing equations

Simulation of a flow field includes the conservation in mass, momentum, and energy described by the continuity equation (1), the Navier-Stokes equation (2), and the total energy equation (3).

Mass conservation equation:

$$\frac{\partial \rho}{\partial t} + \nabla \cdot (\rho \vec{V}) = 0, \quad (1)$$

where t is time, ρ is the instant density, \vec{V} is the instant velocity vector.

Momentum conservation equation:

$$\frac{\partial}{\partial t} (\rho \vec{V}) + \nabla \cdot (\rho \vec{V} \vec{V}) = -\nabla p + \nabla \cdot \bar{\bar{\tau}} + \vec{F}, \quad (2)$$

where p is the pressure, $\bar{\bar{\tau}}$ is the stress tensor, \vec{F} is the additional force per unit volume.

Energy conservation equation:

$$\frac{\partial}{\partial t} (\rho \epsilon) + \nabla \cdot (\vec{V} (\rho \epsilon + p)) = \nabla \cdot (k \nabla T + \bar{\bar{\tau}} \cdot \vec{V}) + S, \quad (3)$$

where k is the thermal conductivity including molecular and turbulent thermal conductivity, T is the temperature, S is the source term. Ohmic heating and radiation are included in the source term of the energy equation. ϵ is the total internal energy per unit mass and can be calculated as follows:

$$\epsilon = h - \frac{p}{\rho} + \frac{|\vec{V}|^2}{2}, \quad (4)$$

where h is the enthalpy per unit mass, which is determined by T .

\vec{F} and S were omitted in the present work. However, when incorporating the arc into the simulation based on local thermal equilibrium (LTE) assumption, additional terms including Lorentz forces in momentum equation (additional force), ohmic input and radiation transport in energy equation (source terms) will have to be considered [9].

2.2. Supersonic flow

The flow within a circuit breaker nozzle could reach extremely high speeds resulting in a compressible flow, in which the density of the gas will vary across the medium. The Mach number is a key parameter used to represent flow compressibility and is calculated as follows:

$$M = \frac{u}{c}, \quad (5)$$

where u is flow velocity and c is the speed of sound in the medium.

Typically, in a circuit breaker, most of the nozzle throat area has Mach number values higher than 0.3 where the gas compressible effects need to be considered. A supersonic flow regime has a strong coupling among velocity, pressure, and temperature fields [7].

The ratio between inertial and viscous force indicates whether the flow will be laminar or turbulent and is measured using Reynolds number [10]. In a circuit breaker the inertial forces are dominating over the viscous forces resulting in a less viscous but turbulent flow. Hence, the gas flow is more likely to experience boundary layer separation at the downstream nozzle area due to the increased inertial forces relative to the viscous forces [11].

The flow within a circuit breakers is compressible as well as turbulent. Therefore, the Reynolds-averaged Navier–Stokes (RANS) equations, which express the conservation of mass, momentum and energy for turbulent flows, are used as governing equations [9]. Furthermore, the $k-\varepsilon$ turbulent model was used to simulate the turbulent effect as it has shown reasonable performance for circuit breaker simulation [12]. Given that the maximum temperature in this simulation is below 1000 K, ideal gas law was used to calculate temperature dependent properties.

2.3. Modelling of supersonic flow

2.3.1. Nozzle geometry

The prototype of the circuit breaker used for computations is from the experiments of Benenson and Frind [4]. Figure 1 shows the nozzle structure with upstream and downstream contact. The upstream contact has a round tip with an outer diameter identical to the nozzle throat diameter, while the downstream contact has a hollow tip. The throat is the most narrow area in the nozzle. In fully open position, a distance of 58.5 mm separates the electrodes. The model was built as 2D axisymmetry, and the detailed parameters of the model are shown in Figure 1.

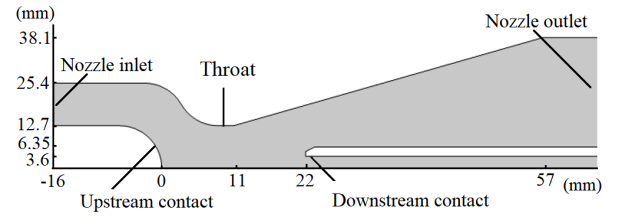


Figure 1. Nozzle geometry.

2.3.2. Boundary conditions

The boundary conditions were specified at the nozzle inlet, the nozzle outlet, the symmetrical axis, and the nozzle wall.

1. The inlet boundary conditions are set up assuming gas in an isotropic process when entering the nozzle. The axial velocity and density are iteratively computed according to the calculated inlet static pressure from a reservoir with stagnation pressure (P_0) and stagnation temperature (T_0).
2. The exit static pressure (P_e) is given as input data in the simulation. The axial gradients of enthalpy and velocity are set to zero. The diffusion of momentum and energy at the exit is negligible compared to the convection and hence ignored in the calculations.
3. The solid surface is considered as a non-slip boundary condition for the velocity. Furthermore, the surface was set to be adiabatic.

A boundary layer mesh was incorporated at nozzle wall and downstream contact to help capture flow structure near wall surfaces [13].

2.3.3. Simulation conditions

The aim of the simulation was to study the capability of the model to predict the supersonic flow within the nozzle. Hence the simulations were conducted without a heat input to the model, and the flow is driven by a pressure gradient between the nozzle inlet and nozzle outlet [7, 9]. The effects of inlet pressure, contacts opening and gas type on the flow structure were studied. Table 1 shows the simulation conditions which were derived from experiments in [12].

Simulation condition	Settings
Inlet pressure P_0 (atm)	11.2, 21.4, 37.5
Opening ratio of contacts	1/3, 2/3, fully open
Gas type	Air, N_2 , SF_6
Outlet pressure (atm)	$0.25P_0$

Table 1. Simulation conditions and settings.

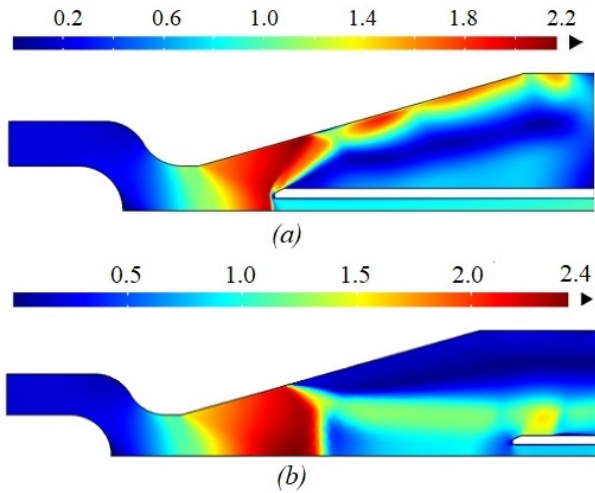


Figure 2. (a) Restricted shock separation, contacts 1/3 open. (b) Free shock separation, contacts fully open. Mach number distribution inside the nozzle with SF_6 as insulation gas and an inlet pressure of 37.5 atm.

3. Results and discussion

3.1. Flow Characteristics in the Nozzle Area

Figure 2 shows Mach number distribution with contacts under partially (1/3rd of fully open) and fully open conditions. Similar to other studies, gas flow starts at subsonic conditions ($\text{Mach} < 1$) at the nozzle inlet, reaching sonic ($\text{Mach} = 1$) conditions at the throat and finally becoming supersonic ($\text{Mach} > 1$) at the downstream area [6, 8]. At a certain distance from the nozzle throat, the Mach number suddenly drops from > 1 to < 1 resulting in a shock. Across a shock, the properties of gas can rapidly change in a very small region, with an almost instantaneously increase of the pressure, temperature, and gas density, and a sharp drop of Mach number and velocity. The shock initially occurs at the tip of the downstream contact and move along with the contact. After a certain contact stroke, it stops moving and stay fixed regardless of the contact location.

Another feature of the shock is the flow separation. Both the shock and flow separation happen at the same time, and they influence the flow state in the nozzle. The flow separation results in a decrease of the effective flow area, which could have a negative influence on arc cooling process, and increase ablation of nozzle wall [14].

When gas flows through a region with an adverse pressure gradient, it flows from the lower pressure area to the higher pressure area. The gas velocity decreases and eventually reaches zero at the wall, which is a separation point. The flow direction changes away from the wall beyond this point.

As shown in Figure 2, the fluid flow slows down in the area behind the shock and at the wall. Hence, its momentum is no longer sufficient to overcome the adverse pressure gradient. This lead to the boundary layer to detach from the surface, resulting in flow

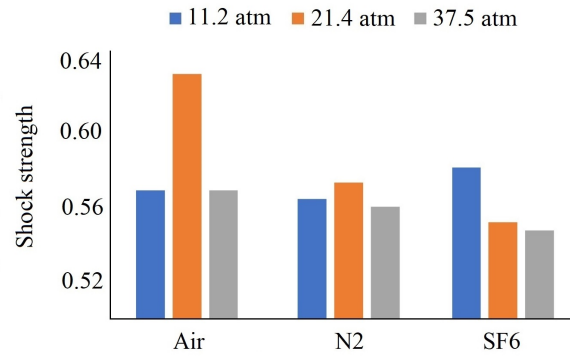


Figure 3. Shock strength for models with Air, N_2 and SF_6 at inlet pressure of 11.2 atm, 21.4 atm and 37.5 atm.

separation.

Depending on the nozzle structure and pressure difference between inlet and outlet of the nozzle, the separation can be classified as two types [11]. One is the restricted shock separation, in which the separated flow reattaches to the wall, forming a closed circulation bubble downstream of the shock as shown in Figure 2(a). Under this condition the shock is strong enough to cause the gas flow to reattach to the downstream wall. The pressure gradient created by the shock can push the gas flow back towards the wall, reattaching it. The other type is the free shock separation, where the separated flow does not reattach to the wall, creating a separation zone that extends all the way to the exit of the nozzle, allowing the gas flow backwards to the separated region [14]. Figure 2(b) shows a free shock separation in which the boundary layer permanently separates from the nozzle wall.

In the initial stages of contact opening, a restricted shock separation occurs in the downstream area of the nozzle. However, with the increase in opening distance, the flow separation becomes a free shock separation.

3.2. Shock strength and flow separation angle

The impact of gas type and inlet pressure on the shock strength was further investigated. The shock strength was defined as the ratio between the increase in pressure across the shock and the inlet pressure [15]. Figure 3 shows the shock strength with different gas types and inlet pressures. For the same inlet pressure, the higher shock strength indicates a higher drop of velocity across shock, which would hinder the convective cooling in the region after shock area. At higher inlet pressure, SF_6 has a lower shock strength compared to other gases and hence has a higher Mach number after the shock. This indicates that under arc conditions, SF_6 might have better cooling performance in the region after the shock.

Furthermore, When the flow separates from electrode and wall, the flow velocity rapidly drops in the downstream region after separation and the Mach

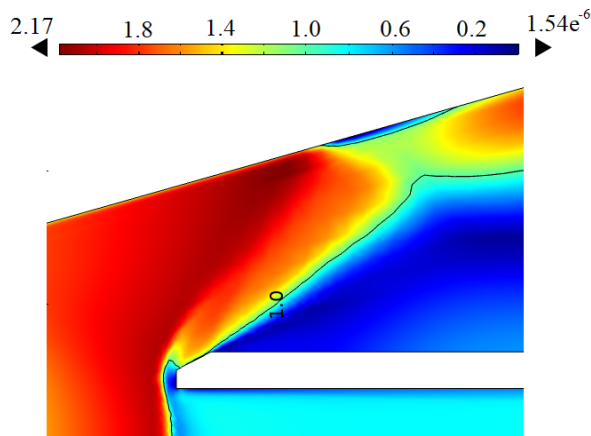


Figure 4. Measurement of flow separation angle of Mach number distribution of SF_6 at inlet pressure of 37.5 atm, 1/3rd open.

number drops to less than 1. This flow separation will result downstream in two flow regimes; a supersonic region and a subsonic region. The supersonic region, here also named effective flow area, decreases in the downstream direction. The decrease of effective flow area will lead to lower convective heat transfer. Therefore, the flow separation angle is measured between the solid surface and the line of Mach 1, as shown in Figure 4. When the contact opening is 1/3rd of the fully open condition, the flow separation occurs at the contact, while under fully open condition it occurs at the wall. Hence the angle is measured either against the contact or wall depending on which of these conditions occurs. Figure 5 shows the flow separation angles for different gas types obtained at 1/3rd and fully open conditions. The larger the separation angle, the smaller the effective flow area, which will lead to poor heat convection in the downstream nozzle area. In both 1/3rd and fully open conditions, SF_6 has the lowest separation angle and air has the highest separation angle. In fully open conditions SF_6 was about 24% lower than air which had the largest angle.

Overall, with the contact opening the shock first separates from contact surface, then flow separates from wall. When the gas flow separates from the nozzle wall, the recirculating flow caused by flow separation can help to mix the gas and facilitate the cooling of the corresponding portion of the arc [14]. However, if the flow separation is not accurately captured in simulation, the efficiency of the arc cooling process may not be correctly represented. Therefore, the behavior of different gases with respect to the shock-induced flow separation as a function of the contact distance, needs to be considered when designing arcing zones for efficient fluid flow and heat transfer.

4. Conclusion

A simulation model was built to study the flow characteristics in a 'de Laval' nozzle used in gas circuit breakers. The study was focused on flow characteristics un-

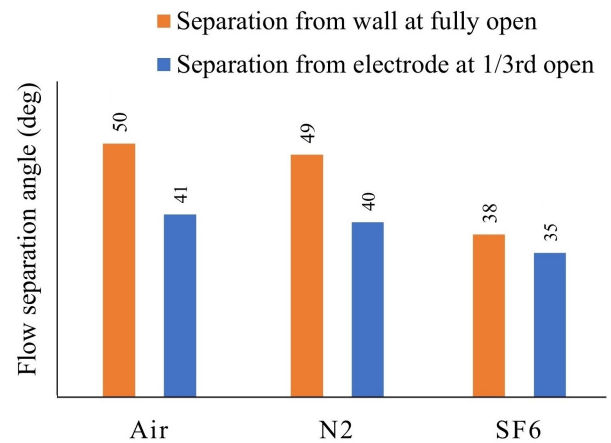


Figure 5. Flow separation angles for N_2 , SF_6 and air at inlet pressure of 37.5 atm and for 1/3rd and fully open conditions.

der cold flow conditions (without arc). The Reynolds-averaged Navier–Stokes equations were solved with $k-\varepsilon$ as the turbulence model. The model successfully simulated the special features characterizing the flow in this type of nozzles, including shocks and flow separations. Furthermore, the developed model was used to compare three different gases – air, N_2 and SF_6 – in terms of shock strength and flow separation angles. The results indicated that gas properties, including dynamic viscosity, specific heat ratio and density, affect the flow characteristics within the nozzle.

References

- [1] H. Ito. *Switching Equipment*. CIGRE, Paris, France, 2019. ISBN 978-3-319-72537-6. doi:10.1007/978-3-319-72538-3.
- [2] M. S. Claessens, R. G. L. Drews, M. Holstein, and H. Lohrberg. Advanced modelling methods for circuit breakers. In *CIGRE*, volume 21, 2006.
- [3] M. Eves. A literature review on SF_6 gas alternatives for use on the distribution network. Report, Western power distribution, 2018.
- [4] D. M. Benenson, G. Frind, R. E. Kinsinger, et al. Fundamental investigation of arc interruption in gas flows. Report, General Electric Company, 1980.
- [5] H. Gremmel. *Switchgear Manual*. ABB, 10th edition, 1999.
- [6] J. F. Zhang and M. T. C. Fang. Dynamic behavior of high-pressure arcs near the flow stagnation point. *IEEE Transactions on Plasma Science*, 17:524–533, 1989. doi:10.1109/27.32266.
- [7] J. J. Gonzalez and P. Freton. Flow behavior in high-voltage circuit breaker. *IEEE Transactions on Plasma Science*, 39(11):2856–2857, 2011. doi:10.1109/TPS.2011.2129538.
- [8] S. K. Park, K. Y. Park, and H. J. Choe. Flow field computation for the high voltage gas blast circuit breaker with the moving boundary. *Computer Physics Communications*, 177:729–737, 2007. doi:10.1016/j.cpc.2007.07.004.

- [9] Q. Zhang, J. D. Yan, and M. T. C. Fang. The modelling of an SF₆ arc in a supersonic nozzle: I. cold flow features and dc arc characteristics. *Journal of Physics D: Applied Physics*, 47(21):215201, 2014. doi:10.1088/0022-3727/47/21/215201.
- [10] H. W. Klink, A. Marinescu, and D. Truta. Cold flow simulation of a 123 kV SF₆ puffer circuit breaker. In *Proceedings of the 6th International Conference on Optimization of Electrical and Electronic Equipments*, 1998. doi:10.1109/OPTIM.1998.710426.
- [11] P. K. Chang. *Separation of Flow*, book section VI – Compressible Flow Separation, pages 210–271. Pergamon, 1970. ISBN 9781483181288.
- [12] J. Mantilla, C. Franck, and M. Seeger. Measurements and simulations of cold gas flows in high voltage gas circuit breakers geometries. In *Electrical Insulation, 1988., Conference Record of the 1988 IEEE International Symposium on*, pages 720 – 723, 2008. doi:10.1109/ELINSL.2008.4570431.
- [13] X. Y. Ye and M. Dhotre. Cfd simulation of transonic flow in high-voltage circuit breaker. *International Journal of Chemical Engineering*, 2012:1–9, 2012. doi:10.1155/2012/609486.
- [14] P. K. Chang. *Separation of Flow*, book section VII – Characteristics of Separated Flows, pages 272–335. Pergamon, 1970. ISBN 9781483181288.
- [15] D. Serre. *Handbook of Mathematical Fluid Dynamics*, volume 4, book section Chapter 2 – Shock Reflection in Gas Dynamics, pages 39–122. North-Holland, 2007. ISBN 9780444528346.